RGNZ/*MGPB*

Determining Rock Fragment Size Distribution Using a Convolutional Neural Network

Elmira Sharifi[1]; Mohamad Ali Ebrahimi Farsangi[2]; Hamid Mansouri[3]; Esmat Rashedi[4]

[1] Mining Engineering Department, Shahid Bahonar University of Kerman, Iran, Lm.sharifi@yahoo.com

[2] Mining Engineering Department, Shahid Bahonar University of Kerman, Iran, maebrahimi@uk.ac.ir

[3] Mining Engineering Department, Shahid Bahonar University of Kerman, Iran, hmansouri@uk.ac.ir

[4] Department of Electrical and Computer Engineering, Graduate University of Advanced Technology, Kerman, Iran, e.rashedi@kgut.ac.ir

Abstract

Fast and relatively accurate determination of the fragment size distribution of a muck-pile is still a challenge in mining operations and the existing measurement methods are inefficient. In this research, a new algorithm to determine fragment size distribution due to blasting was presented, using the image processing technique. In the newly proposed approach, delineating of the fragmented rock particles, as the main core of processing, was carried out, using a convolutional neural network. Two networks were defined and trained by 150 laboratory and 150 field data images. Also, 30 laboratory and 30 field data images were applied to carry out the validation visually, and by using F1-scores. For the two laboratory and field networks and results obtained by Split-Desktop software automatic edge detection on the same images, the F1-scores are equal to (0.98, 0.74) and (0.99, 0.85) respectively. Also, for determination of fragment size distribution by laboratory data network and Split-Desktop software automatic edge detection on the same images, the Root Mean Square Error (RMSE) for F30 and F80 are equal to (0.36, 1.20) and (0.31, 1.24) respectively. These indicate better performance of the proposed approach for both rock edge detection and fragment size distribution over Split-Desktop software automatic edge detection.

1. Introduction

Due to the important role of rock fragment size on all stages of mining operations, including loading, hauling, and crushing, it is necessary to provide an accurate, fast and low-cost method to determine the fragment size distribution (**Bhattacharya and Chandrakar, 1999; Siddiqui et al., 2009; Hudaverdi et al., 2012; Sanchidrián et al., 2012; Faramarzi et al., 2013**). The existing measurement methods to determine the fragment size distribution are generally classified into direct and indirect categories. The direct method is sieving and its results are the most accurate, but it is time-consuming and very expensive. Also, it is rarely possible to use it because of disturbing the mining and production process. Indirect methods include the oversize boulder count method (manual counting of the oversize boulders in the muck-pile, which cannot be loaded by the shovel. In this method, an oversize index is defined based on the total blasted rock mass), consumption of explosive in the sec-

ondary blasting (an index is introduced based on the used explosives in the secondary blasting), shovel loading rate method in which the speed of loading is a sign of good fragmentation, delays due to bridging in the crusher, which is mainly due to big boulders, visual analysis method (assessment of muck-pile immediately after blasting), photographic or manual analysis method, which is based on the delineation of fragments in muck-pile photographs, high speed photography or image analysis method in which digital images of the blasted rock were used to determine size distribution of muck-piles (**Roy, 2005**). Up to now, applying indirect methods, specifically methods based on image analysis techniques to determine the size distribution of fragments, has become an efficient solution with the least disturbing of the production cycle. The general procedure of these methods is taking photos from the fragmented rocks, and then edge detection of each particle (fragments) in the photos is done manually or automatically. Finally, the fragment size distribution is estimated, using computational techniques. Obviously, in this process, the accurate edge detection of fragments has a main role in obtaining correct results (**Wu and Kemeny, 1992; Sudhaka et al., 2006;**

Corresponding author: Mohamad Ali Ebrahimi Farsangi

e-mail address: maebrahimi@uk.ac.ir

Han and Song, 2014; Sereshki et al., 2016; Yaghoobi et al., 2019). The first rock particle size estimation system based on image processing technique including edge detection and measuring the particle arc chord was presented by Gallagher (**Gallagher, 1976**). Also, an image analyser system was developed by Nyberg et al. to scan the particle chord size of edge detected muck-pile images (**Nyberg et al., 1983**). Furthermore, the image processing technique was used as an automatic method to determine the rock fragmentation by separating touched and overlapped particles (**Maerz et al., 1987**). In addition, in 1991, to estimate the sieve size and the volume of fragmented rock, a modern method was developed, using techniques of digital image processing. In this research, delineating of the fragmented rock was done by using filters that enhance the edges by weighting components with high frequency of the transformed image (**Farmer et al., 1991**). Moreover, in 1992, an automatic particle segmentation system was presented by Wu et al. to estimate the fragment size distribution. In the proposed algorithm, the Sobel gradient filter was used for shape recognition and to separate rock particles from shadow boundary convexity points and finds clusters of rock particles (**Wu and Kemeny, 1992**). In addition, in 1993 Lin et al. proposed a segmentation algorithm, using edge detection techniques to identify each particle. In this method, sieve size distributions were estimated based on the measured chord-length of each particle (**Lin et al., 1993**). Also, Kemeny proposed an algorithm in which the Sobel gradient filter was used for particles' edges detection and for size estimation, elliptical approximation was used (**Kemeny, 1994**). Moreover, in 1996, the Split software based on image analysing was presented for calculating the fragment size distribution. In this study, the Sobel gradient filter was used to delineate the rock particles, and the Watershed algorithm was applied for separating different objects in an image and segmentation the particles. Determination of the fragment shape and computation of the size distribution was carried out, using empirically derived statistical equations (**Girdner et al., 1996**). Furthermore, Maerz et al. developed an automated granulometry tool to estimate size distributions named WipFrag by using a digital image of rock particles and optimizing Edge Detection Variables (**Maerz et al., 1996**). Also, in 1998 Yen et al. in used the Watershed algorithm for rock particles segmentation (**Yen et al., 1998**). In addition, in 1998 Wang presented a heuristic algorithm to split the rock particles. In this algorithm, by using a cost function and assigning a polygonal approximation for each object, the fragment boundaries were detected (**Wang, 1998**). Also, in 2005, a method was presented to measure the rock particle size. In the mentioned method, the edge of each particle was detected using, a one-pass edge detection algorithm and the average size was estimated based on the image edge density (**Wang and Bergholm, 2005**). Moreover, in 2007 Al-Thyabat et al. used the Watershed

algorithm to split overlapped rock particles and then measured two different dimensions of each particle to determine the fragment size distribution (**Al-Thyabat et al., 2007**). Also, in 2008 Wang developed three segmentation algorithms based on edge detection, split-and-merge, and thresholding techniques along with a method for splitting overlapping particles (**Wang, 2008**). In addition, in 2008 Thurley and Andersson presented a tool for measuring the size of iron ore pellets, using the morphological image segmentation technique (**Thurley and Andersson, 2008**). Furthermore, in 2011 Thurley developed a fully automated online system to measure the rock particle size distribution, by using morphological edge detection technique in 3D data analysis (**Thurley, 2011**). Moreover, mathematical morphology technique was applied to segment the existing micro-cracks on sandstone microscopic images (**Obara et al., 2011**). Also, in 2011, Ko and Shang improved a prediction model to determine the size distribution of ore particles based on the obtaining, the uniformity of particles, using surface images and a neural network (**Ko and Shang, 2011**). Also, in 2012 Zhang et al. described an approach, using image segmentation on overlapped coal particle images (**Zhang et al., 2012**). In this research, in order to detect the boundaries of particles, the thresholding Otsu method (**Otsu, 1979**) was used and the images were proceeded, using an exponential high pass filter, Fourier transform and a morphological technique was used for edge detection. Moreover, neural networks were used to determine the crushed material size distribution. In this research after imaging and segmenting, the size features were extracted and finally by using the integrating Principal Component Analysis (PCA) and neural network, the size distribution of each image was estimated (**Hamzeloo et al., 2014**). Also, Bull et al. presented a method for segmentation of rock fragments, by Haar-like filtering of digital images (**Bull et al., 2015**). Moreover, Sereshki et al. used the Sobel filter and mathematical morphology to develop an algorithm to detect the edges of fragments (**Sereshki et al., 2016**). Furthermore, in 2016, a delineation algorithm was developed in which by using stereophotogrammetry, blocks were modelled in three dimensions and delineated based on the geometrical features (**Han and Song, 2016**). Also, Karimpouli and Tahmasebi presented a deep convolutional autoencoder network (SegNet) to segment the digital rock images, which was used in Digital Rock Physics (DRP). According to the evaluation of the obtained results, the proposed algorithm is more efficient than the multi-phase thresholding method (**Karimpouli and Tahmasebi, 2019**). In addition, Rahmani et al. presented an automatic segmentation system to estimate the volume, weight and the size distribution of gravel particles. The proposed method is based on 3D scanning and a surface reconstruction algorithm (**Rahmani et al., 2019**). Furthermore, Jang et al. developed a 3D rock fragment measurement system based on photogrammetry (**Jang et al., 2020**). Also, Yang et al. suggested the

image processor toolbar of MATLAB software to calculate the coal particle size. The performed image analysing techniques can be summarized in the stages of binarizations, segmentation, noise elimination, sharpening, contrast enhancement, and the use of the edge preservation filter, scale calibration and fragment size measuring, using intermediate axis of fitted ellipse (**Yang et al., 2020**). Furthermore, a convolutional neural network (Alexnet) was modified in 2021 by Yang et al. for the classification of fragments. In this research, the images of the rock fragments were captured by the mounted camera above the conveyor belt and then classify based on the largest fragments. The results showed that the modified model has good performance (**Yang et al., 2021**). Also, in 2021 Bamford et al. used a deep neural network (DNN model) to measure the size of rock fragments. In this work muck- pile images were analysed and the results showed that the proposed model is fast and has acceptable accuracy in size prediction (**Bamford et al., 2021**). In addition, four intelligent models were proposed to estimate the fragments size distribution. These models were obtained by combining of firefly algorithm with machine learning algorithm including gradient boosting machine, support vector machine, Gaussian process and artificial neural network. Each model was optimized, using the results of fragment images analysing by Split-Desktop software. The results demonstrated that among the proposed models, the combination of firefly algorithm with gradient boosting machine is the most accurate and has more reliable results (**Xie et al., 2021**). Also, in 2021 Bai et al. proposed a method based on the Watershed algorithm, the K-nearest neighbour algorithm, and the Convex shell method to segment the coal particle and determine the size distribution of coal particles (**Bai et al., 2021**). Furthermore, a DexiNed convolutional neural network was modified by Li et al. in 2021 to determine the size distribution of aggregates on the conveyors in a crushing plant, by edge detection of rock particles images (**Li et al., 2021**). Moreover, Li et al. developed an approach to estimate the size distribution of metallurgical cock. In this algorithm to detect the cock particles an object detection deep learning algorithm named Yolov3 was used. Size distribution estimating was done by measuring the width of bounding box as particle size and size conversion. Error correction was done by using the results of cock sample sieving. The results showed that the particle detection model is accurate and fast (**Li et al., 2022**).

By now, the Split system (Split-Desktop) is the most common software used to estimate the fragment size distribution. Using this software, rock particle delineating can be done in manual and automatic modes. Manual delineating is very time-consuming and its automatic mode, which is based on classical image processing algorithms such as Sobel and Watershed, does not have good performance in correctly detecting rock particle edges. The main objectives and contributions of this research is to determine fragment size distribution more

accurately and fast by enhancing the edge detection of rock particles, by using one of the most advanced deep learning techniques called Convolutional Neural Networks (CNN). However, the errors due to 2D analysis and overlapping still exist.

Deep learning algorithm, as a type of machine learning algorithm, is an artificial neural network with hierarchical architecture, including multiple processing layers to extract conceptual and high level features progressively (**Guo et al., 2016**). Different architectures of deep learning algorithm have been used in different fields of researches such as speech recognition (**Abdel-Hamid et al., 2013**), medical image analysis (**Li et al., 2014**), computer vision (**Luo et al., 2018**), natural language processing (**Li et al., 2019**), machine translation (**Meng et al., 2015**), bioinformatics (**Zeng et al., 2016**), material inspection (**Weimer et al., 2016**), and drug design (**Francoeur et al., 2020**). Convolutional neural network is a special architecture of deep learning algorithm. In this research, in order to design rock edge detection network, Convolutional Neural Network (CNN) is used because of its popularity and excellent performance in image pattern recognition (**Gu et al., 2018**).

CNN architecture is a combination of deep neural networks with convolutional filters, which are organized in different layers and connected, using weights and biases. This network has different architectures depending on various objectives. Typically, it consists of a convolutional layer, a pooling layer, and a fully connected layer or a 1×1 convolution layer in the last layer to achieve high-level reasoning or classifying (**Wang, 1998; Lin et al., 2013; Petersen et al., 2014; Gu et al., 2018; Kattenborn et al., 2021**). The convolutional layer as the main core of the CNN, consists of multi optimizable filters, which convolve the input by 2D or 3D moving along it to extract features. Then, to generate 2D or 3D feature maps, activation function is used. Relu, Sigmoid, and Tanh are the most common activation functions used. The depth of each convolutional layer output is equal to the number of generated feature maps. Pooling as a reduction operator has no trainable parameters and its main purpose is effective sampling to reduce the dimensions of the obtained feature map, while preserving important data. It is usually placed between two convolutional layers. The most common pooling are max pooling and average pooling. A fully connected layer involves weights, biases, and neurons. These neurons are fully connected to all activation functions of previous layers. It is used for image classification.

In this research, CNN is used to predict the label of each pixel (edge or non-edge). To train the network, datasets consist of input and target data are required.

2. Materials and Methods

In this research, two laboratory (lab) and field datasets were prepared to train and test CNN networks.

Then, based on the purpose of the research, the network's architectures were designed.

2.1. Data collection

In order to prepare lab datasets, 8 ASTM E11 standard sieves (see **Figure 1a**) with aperture size 4, 3.5, 3, 2.5, 2, 1.5, 1, 0.5 inch were used to classify the various sizes rock particles (sands and gravels) into seven size categories A to G (see **Table 1**).

**Table 1:** The specifications of size categories

Size Category	The Sieve Aperture Size (inch)	
	Passed through	Retained on
A	4	3.5
B	3.5	3
C	3	2.5
D	2.5	2
E	2	1.5
F	1.5	1
G	1	0.5

Rock samples were prepared by the mixing of rock particles belonging to each size category according to pre-designed weight patterns and the lab datasets were collected by 2D imaging from mixed samples. All images were captured under standard laboratory conditions in image processing laboratory of Mining Engineering Department of Shahid Bahonar University of Kerman, Iran. Each image belongs to a unique weight pattern, which is a mixture of different size categories. To have the same dimension for all images, a scaled square frame (see **Figure 1b**) with dimensions of 60×60×5 cm was used, and rock particles placed inside it. Also, a frame with a height of one m (see **Figure 1c**) was used to keep the distance between the camera and the centre of imaging surface constant, in which the camera was installed on top centre. In order to provide a constant brightness of at least 700 lux, the laboratory was light isolated, and two LED bulbs were used as the source of light (see **Figure 1c**). Totally 180 mixtures of sands and gravels were designed and the corresponding images were taken. One of the pre-designed mixture weight patterns is given in **Table 2**.

The field datasets were collected by 2D imaging from the muck-piles of fragmented rocks by blasting (180 images were taken) at the Sarcheshmeh copper mine. The Sarcheshmeh copper mine with a daily production of 100,000 tones is a porphyry deposit, with a reservoir of about 1.2 billion tones, located 160 km southwest of Kerman, Iran.

For both lab and field images, to prepare training and testing dataset (input and target data) the original captured images were pre-processed by cropping and converting to grayscale to use as input data. To prepare the target data (label), edge detection was done manually
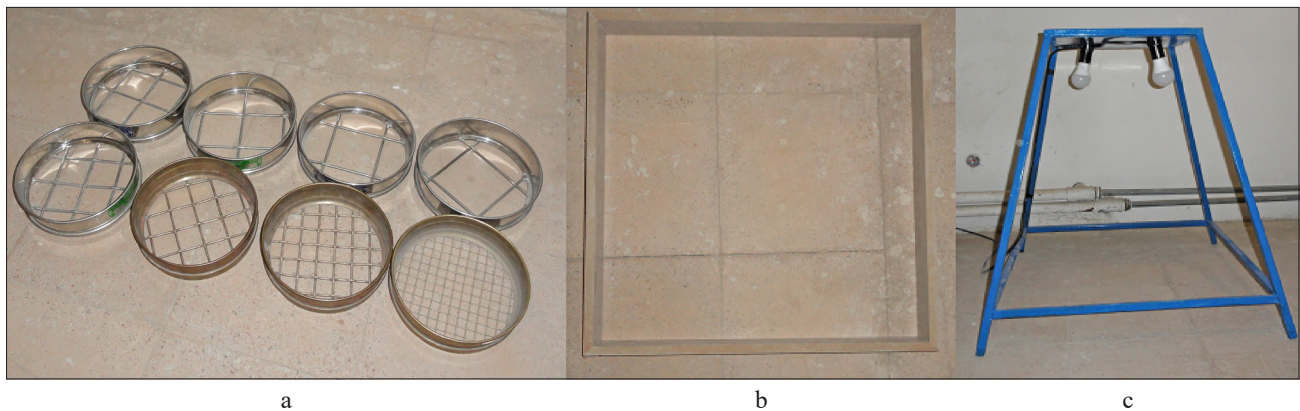
Figure 1: The tools used for lab imaging: (a) ASTM E11 standard sieves, (b) square frame, (c) frame with height of one m

Table 2: One of the pre-designed weight patterns

| Size Categories	Weight (%)	Weight (kg)
A	26	7.2
B	14	3.8
C	34	9.3
D	9	2.5
E	8	2.2
F	6	1.7
G	3	0.9

and a band of edge detected image was extracted and used as target data. **Figure 2** and **Figure 3** show an example of the original captured images (a), pre-processed image (b), manually edge detected (c), and target data (d) belongs to the lab and filed datasets respectively.

2.2 Rock edge detection network architecture

In this paper, to detect the rock particles edges, the convolutional neural network with U-shape architecture (U-net) proposed by Ronneberger et al. (2015) applied for biomedical image segmentation, was used. Accurate
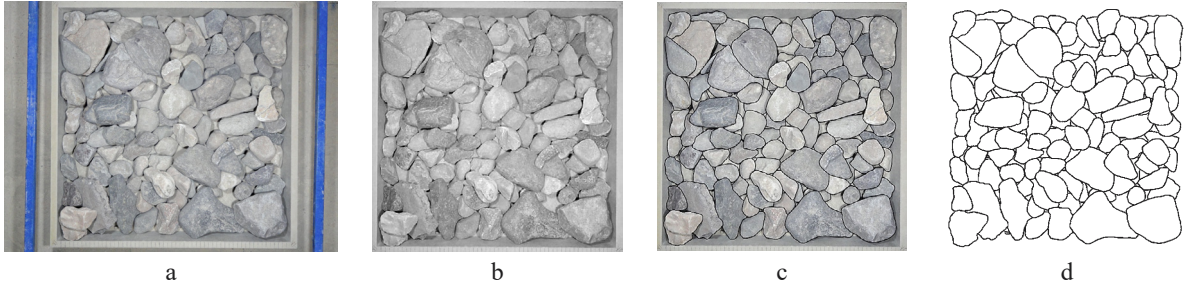
Figure 2: Preparation of input and target data of the laboratory dataset: (a) Original captured image, (b) Image after pre-processing (input data), (c) Manually edge detected image, (d) Target data (a band extracted from image c).
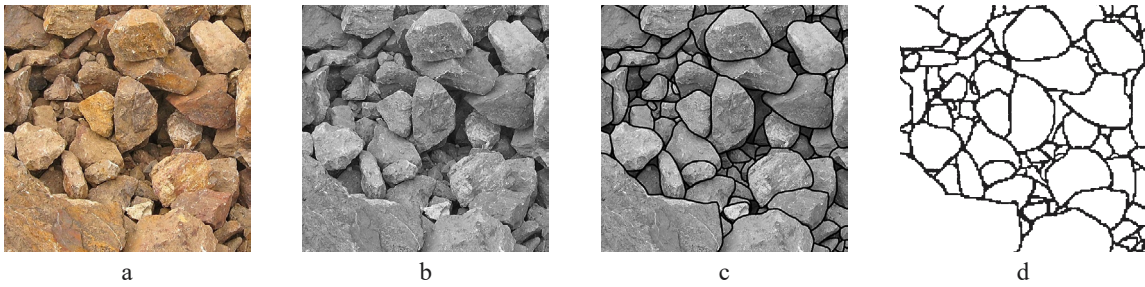
Figure 3: Preparation of input and target data of the field dataset: (a) Original image, (b) Image after pre-processing (input data), (c) Manually edge detected image, (d) Target data (a band extracted from image c).

Table 3: The details of U-nets used for lab and field datasets

Dataset	The network architecture	The total number of convolution layers	The number of trainable parameters (in millions)
Lab	64(2)→128(2)→256(2)→512(2)→256(2)→128(2)→64(2) → 2(1)→1(1)	18	7.69
Filed	64(2)→128(2)→256(2)→512(2)→1024(2)→512(2)→256(2) →128(2)→64(2)→2(1)→1(1)	23	31.03
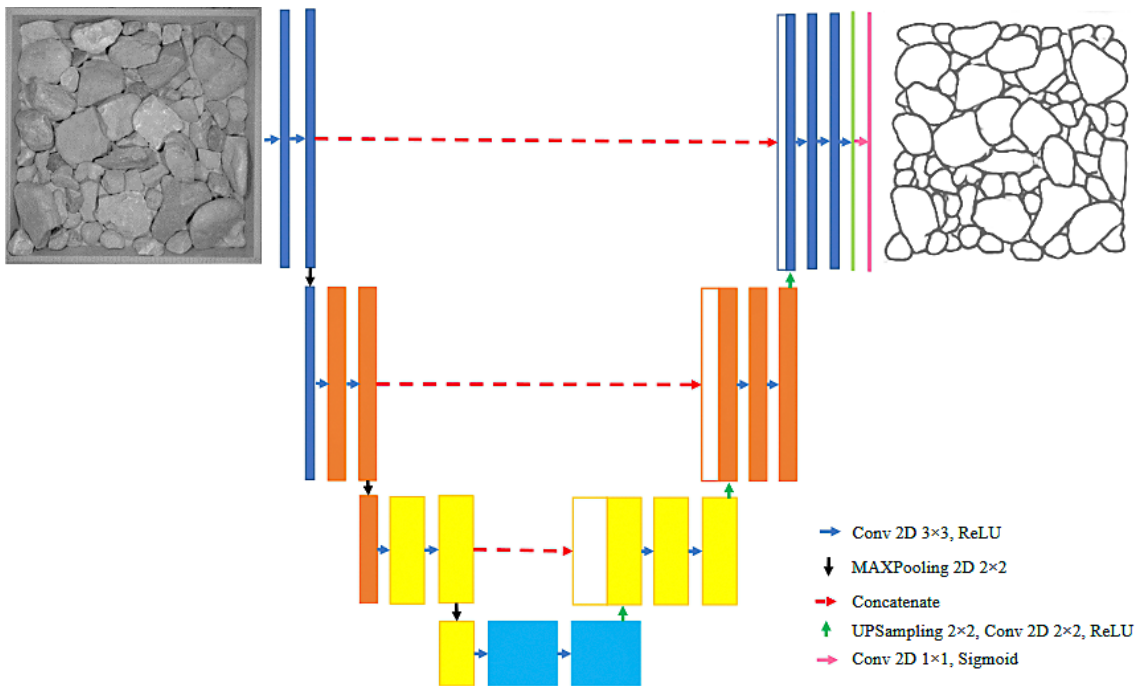
Figure 4: The U-net architecture for the lab dataset (after **Ronneberger et al., 2015**)
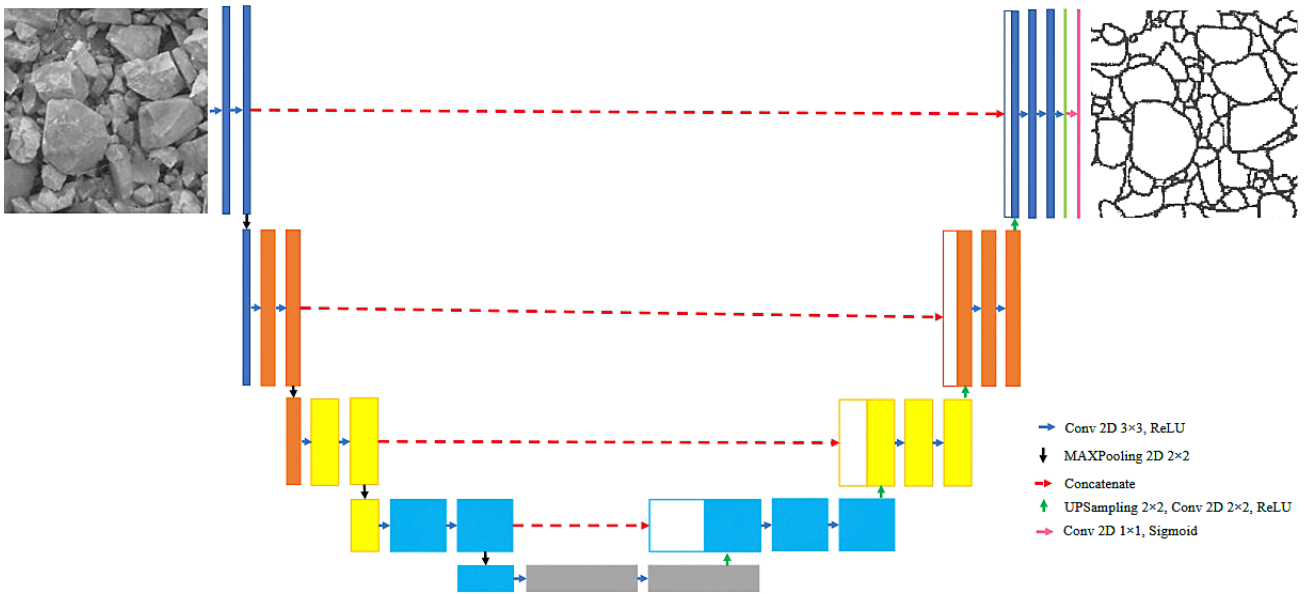
Figure 5: The U-net architecture for the field dataset (after **Ronneberger et al., 2015**)
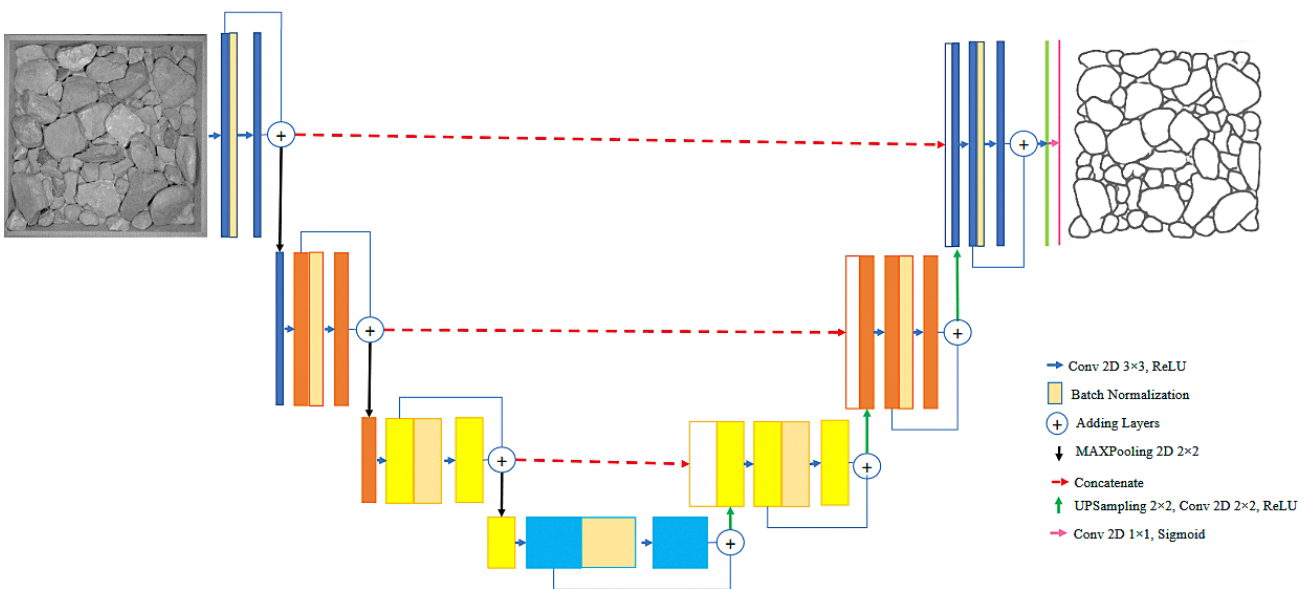

Figure 6: The modified U-net architecture for the lab dataset
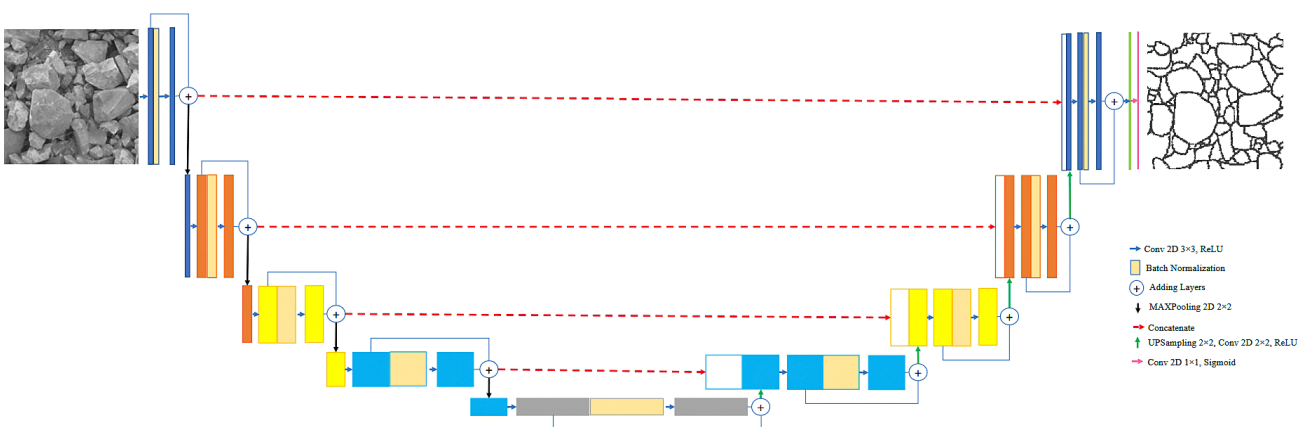

Figure 7: The modified U-net architecture for the field dataset.

and efficient results in the image pixel-wise classification were obtained by using this network. Also, U-net has good performance with training data (**Ronneberger et al., 2015; Shamsolmoali et al., 2019; Sivagami et al., 2020; Gore et al., 2022**). The U-net architecture consists of two contraction and expansion paths, including convolutional layers. The main difference between these two paths is the use of pooling operators in the contraction and up-sampling operators in the expansion path. In this network, in the last layer, a 1×1 convolutional layer is used, followed by a Sigmoid function as an activation function. Also, in the U-net, in each convolutional layer, the same padded 3×3 convolution filters with Rectified linear unit (Relu: max (0, X)) as an activation function, applied twice repeatedly and then transferred to the pooling layers. The same padding technique by adding the zero value layers around the input image prevents the size reduction due to convolution. In the contraction part of this network, 2×2 max pooling with stride 2 is used to down sample after convolutional layers. In the expansion path, the up-sampling operator is used. It multiplies the dimensions of input and followed by convolutional layer. There are various up-sampling techniques, among them the nearest neighbour is the most common. In the expansion part of the proposed network, to increase the output spatial resolution and localize it, 2×2 up-sampling (nearest neighbour) is used followed by a 2×2 convolutional layer. Then, the high-resolution feature maps obtained from the contracting part are merged with up-sampled outputs correspondingly. The U-net was used for both lab and field datasets (see **Figure 4** and **Figure 5**). The details of U-nets, in-

cluding the number of convolutional filters (generated feature maps) in each layer with their repetitions, the total number of convolution layers, and the number of trainable parameters is given in **Table 3**.

Also, in this research a modified U-net architecture inspired by the convolutional deep residual network (**He et al., 2016; Targ et al., 2016; Mousavi et al., 2019**) is proposed. In this network the U-net is modified by replacing the two successive convolutional layers with a 2D residual convolutional unit. The U-net architecture was modified for lab dataset (see **Figure 6**) and field dataset (see **Figure 7**). In the convolutional residual unit, a same padded 3×3 convolution filter followed by Relu is applied and normalized, using batch norm. Then, it is convolved again with another same padded 3×3 convolution filter followed by Relu. In this network, to achieve more conceptual features, the outputs of two successive convolutional layers are added and then transferred to the pooling and up-sampling layers. The details of modified U-nets, including the number of convolutional filters (generated feature maps) in each layer with their repetitions, the total number of convolution layers, and the number of trainable parameters is the same as in **Table 3**.
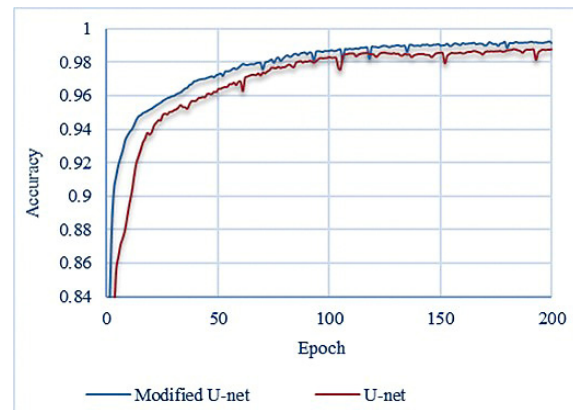
3. Results

The edge detection networks were trained, using lab and field datasets and then evaluated. After image edge detection and identification of rock particles, the size distribution of rock particles for each image was determined and the obtained results were compared with the sieve analysis results for the lab datasets.

Table 4: The details of networks trained

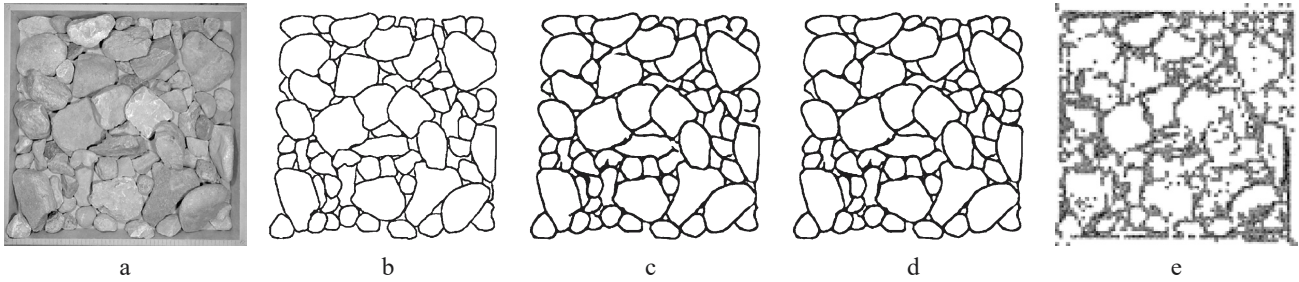| Network | Dataset | | | | | |
| | Lab | | | Filed | | |
	Accuracy	Training time (s/epoch)	Testing time (s/sample)	Accuracy	Training time (s/epoch)	Testing time (s/sample)
U-net	0.9730	640	0.8	0.9928	890	1
Modified U-net	0.9845			0.9856		
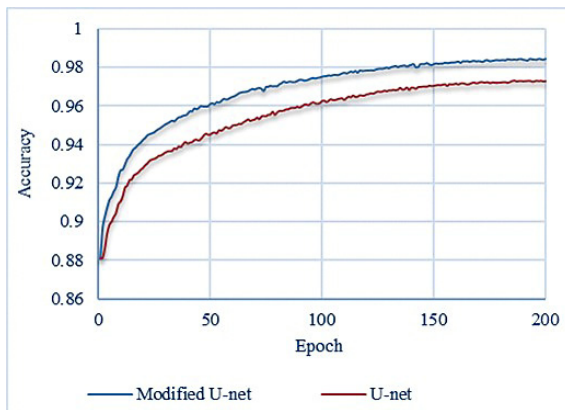
Figure 8: The training accuracy: (a) Lab dataset (b) Field dataset

Figure 9: Performance evaluation of the networks: (a) The original lab image, (b) The result of manual edge detection (ground truth), (c) The result of U-net, (d) The result of modified U-net, (e) The result of Split-Desktop.
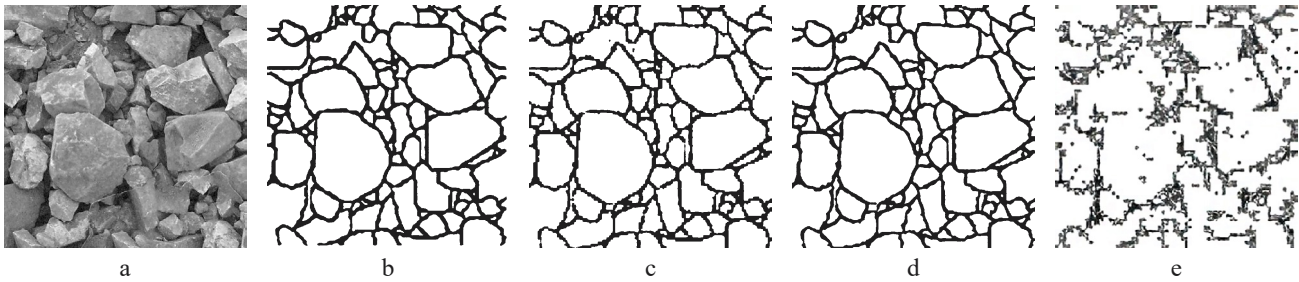
Figure 10: Performance evaluation of the networks: (a) The original field image, (b) The result of manual edge detection (ground truth), (c) The result of U-net, (d) The result of modified U-net, (e) The result of Split-Desktop.

3.1. Networks training

The U-net and modified U-net were trained by both lab and field datasets. For each network, 180 images (256×256) were used of which 150 images were used for training and 30 images for testing. He-Normal method was used for initializing weights and biases. Also, binary cross-entropy as loss function and Adaptive Moment Estimation (ADAM) with a learning rate of 10^{-4} as an optimizer were used. For both datasets, the networks were trained by 200 epochs with batch size of 100. The training accuracy was calculated by **Equation 1 (Csurka et al., 2013; Luo et al., 2019; Romanuke, 2019)**:

$$Accuracy = \frac{T_p + T_N}{T_p + T_N + F_p + F_N} \qquad (1)$$

Where:

TP – True Positive,

TN – True Negative,

FP – False Positive,

FN –False Negative.

The final training accuracy and training and testing times for lab and field datasets for both networks are given in **Table 4**. Also, increasing in the accuracy of training process is visible for lab and field data datasets (see **Figure 8**). According to the achieved results, the training process of the networks was carried out with acceptable final accuracy. However, the modified networks were trained with greater accuracy. The training accuracy, the training time of each epoch, and the test time of each sample are shown in **Table 4**. As it can be observed from this table, by using the proposed models, the edge detection was carried out with high accuracy and the edge detecting time of each image is significantly reduced compared to the manual edge detecting.

3.2. Networks performance evaluation

The performance of trained networks was evaluated, using 30 lab and 30 field test images (not used for training). The approximate time to delineate fragments in each image was estimated at about 0.8 and one second for lab and field images respectively. The performance of U-net and modified U-net were compared with the results of Split-Desktop automatic edge detection and the manually edge detected images (ground truth) on the same lab and field test images.

As an example, the performance of U-net, modified U-net, Split-Desktop automatic edge detection, and the manually edge detected images were compared on the same lab test images (see **Figure 9**) and field test images (see **Figure 10**). As it can be observed from these figures and in fact for all test images, the results achieved through U-net and specially modified U-net for both lab and field test images are significantly more accurate than the results obtained by automatic edge detection of Split-Desktop software and visually close to the manual edge detecting.

Furthermore, to quantify the evaluation, the F1-score was used to measure the matching between the predicted boundary and the real boundary (**Csurka et al., 2013; Luo et al., 2019; Mousavi et al., 2019; Romanuke, 2019**). It is ranging between 0 and 1. If the F1-score is one, it means that there is a full match between the boundary contours of an object in the prediction and ground truth. It can be calculated by **Equation 2**.

$$F1-score = 2 \times \frac{Precision \times Recall}{Precision + Recall} \qquad (2)$$

In this equation, precision is a positive predictive value and is defined as the ratio of the number of points on the prediction boundary, which are very close to the boundary of ground truth to the length of the boundary predicted. It means that the precision is the relation between all elements categorised as positives and true positives (**Equation 3**) (**Csurka et al., 2013; Luo et al., 2019; Mousavi et al., 2019; Romanuke, 2019**).

Table 5: The results of quantitative boundary matching evaluation

Item	Mean F1-score	
	Lab dataset	**Filed dataset**
U-net	0.9842	0.9853
Modified U-net	0.9898	0.9936
Split-Desktop automatic edge detection	0.7446	0.8515

$$Precision = \frac{T_P}{T_P + F_P} \qquad (3)$$

In Equation 2, recall is the ratio of the number of points on the boundary of the ground truth that are very close to the prediction boundary to the length of the ground truth boundary. It means that recall is the relation between all positive elements and true positives, as shown in **Equation 4** (**Csurka et al., 2013; Luo et al., 2019; Mousavi et al., 2019; Romanuke, 2019**).

$$Recall = \frac{T_P}{T_P + F_N} \qquad (4)$$

In this research, the F1-score was computed for both 30 lab and 30 field test images, between the results of the manually edge detected (as ground truth) and the results of U-net, modified U-net, and Split-Desktop automatic edge detection (as prediction) (see **Figure 11** and **Figure 12**). Also, the mean F1-scores of 30 test images for both data-
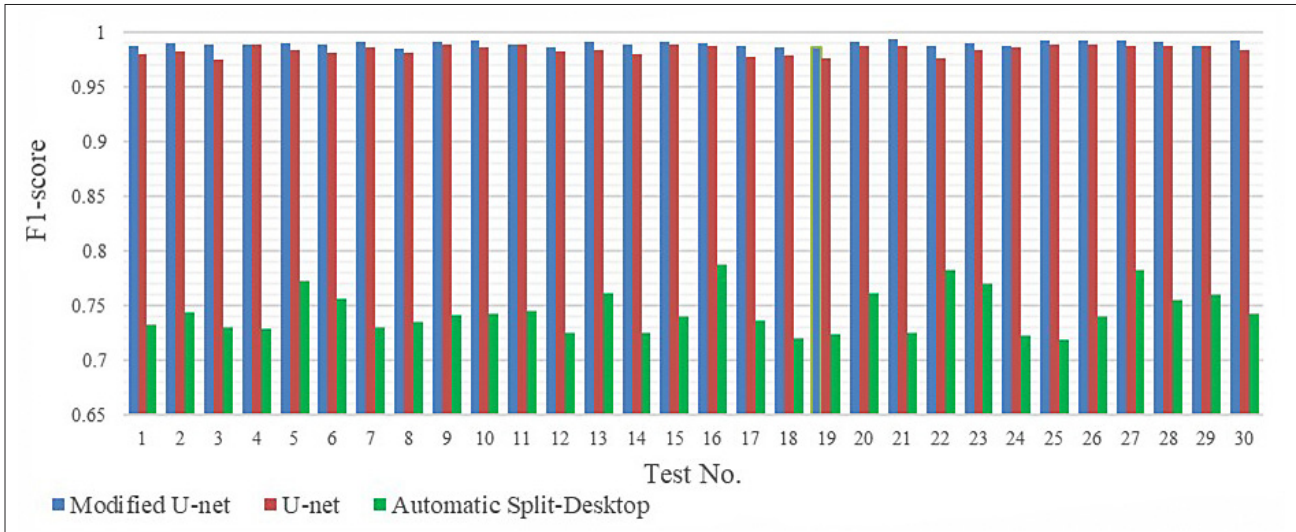
Figure 11: Boundary matching evaluation of the lab test images
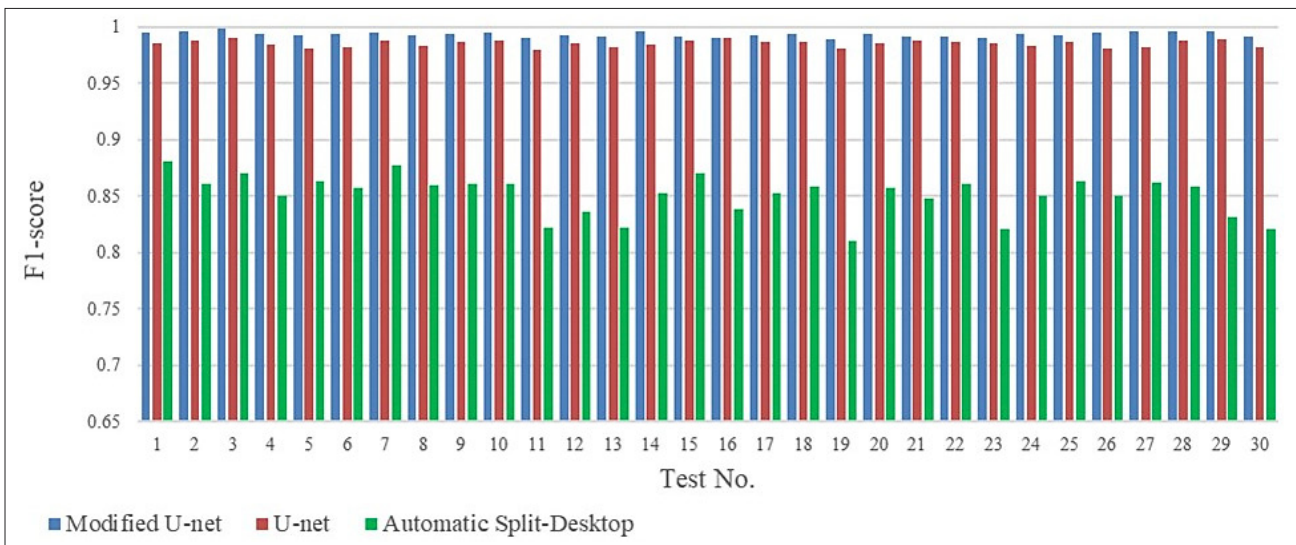
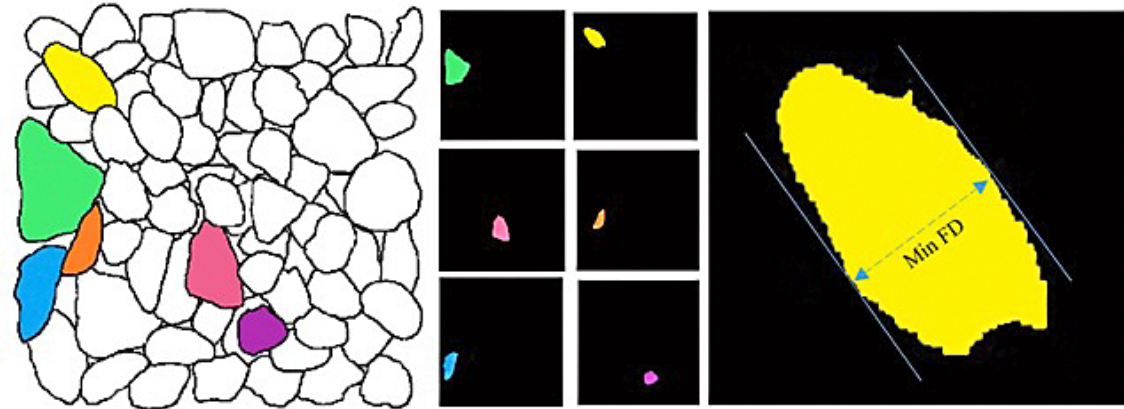**Figure 12:** Boundary matching evaluation of the field test images

Figure 13: The process of rock particle extracting and Min FD measuring
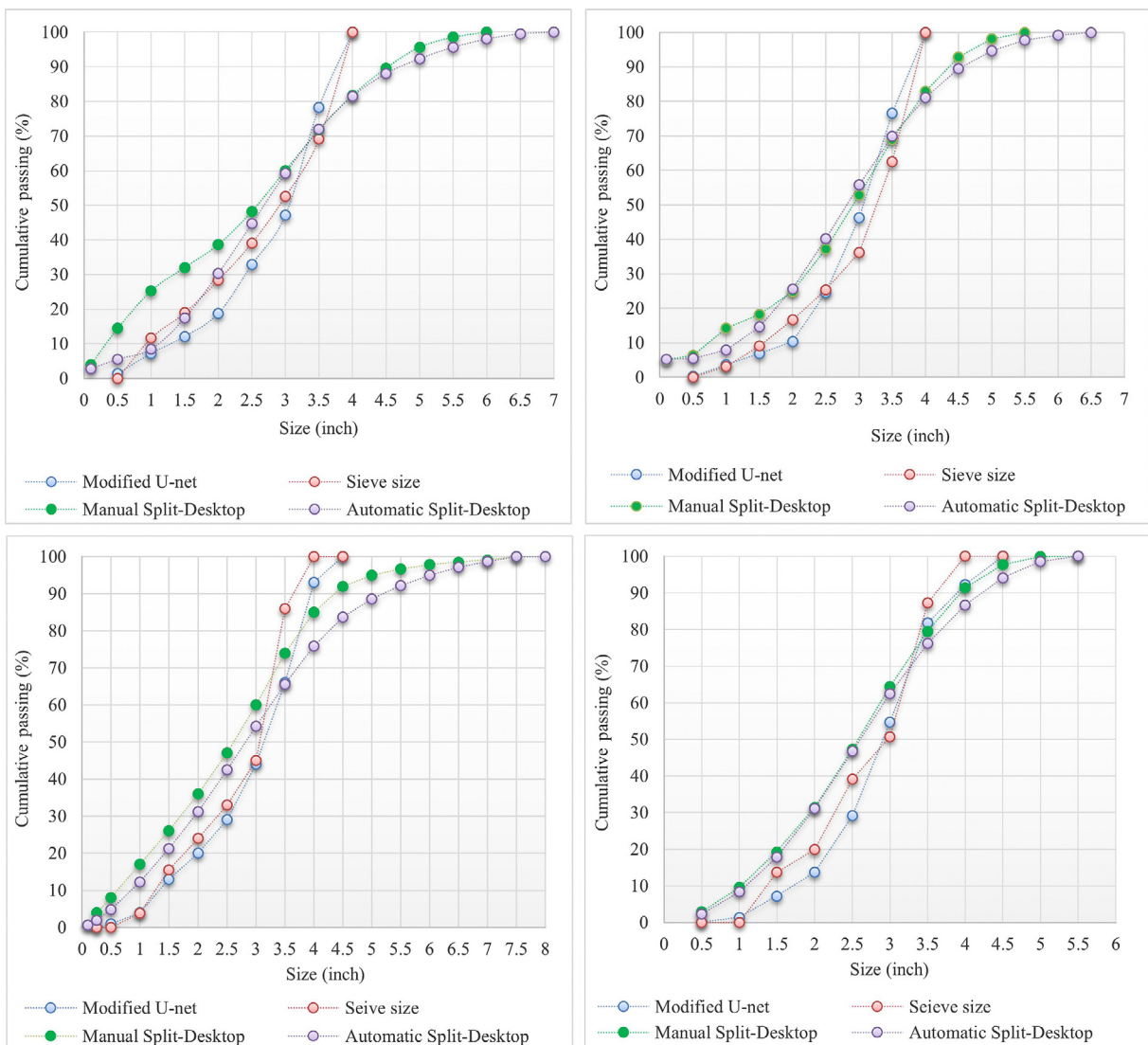

Figure 14: The rock particle size distribution for four lab test images

sets are given (see **Table 5**). As it can be seen from these figures and the table, there is a very good match between the results of 30 manually edge detected lab and field test images and the results of U-net and modified U-net com-

pare to the results of Split-Desktop, which once again confirm the ability of the U-net and modified U-net for rock fragments edge detection. Also, the obtained results demonstrate that the modified U-net with the same number of

Table 6: A quantitative evaluation for 30 test images, using RMSE

Cumulative passing	Modified U-net	Manual Spilt-Desktop	Automatic Split-Desktop
F_{80}	0.31	0.43	1.24
F_{30}	0.36	0.74	1.20

trainable parameters has even better performance (higher accuracy and F1-score) compared to the U-net.

3.3. Determining the rock particles size distribution

By using the modified U-net for particles edge detection, the rock particle size distribution for 30 lab test images was determined and the results compared with the ones obtained by sieving and Split-Desktop (manual and automatic edge detection) for the same test images. To determine the size distribution of particles in each sample (image), it is needed to estimate the sieve size of each detected rock particle in the sample. Therefore, the goal is to measure the maximum diameter of the minimum dimension of the rock particles. For this purpose, the Minimum Ferret Diameter (Min FD), which is the minimum distance between two parallel tangents of an object, is measured as sieve size after extracting the detected rock particles, using the scaled frame. In the Split-Desktop software, particle size is determined, using measurement of the minor and major axis of the best fitted ellipse. However, in the proposed algorithm, using the Ferret diameter is preferred because it is directly measured from the fragment and it is more accurate.

The process of particle extracting and Min FD measuring for one of the lab samples is shown in **Figure 13**. After sieve size classifying of the rock particles, A to G, the volume of each particle is calculated by measuring the area of it and the third dimension is considered equal to the Min FD. In the Split-Desktop software, the third dimension is considered equal to the average of minor and major axes.

The performance of modified U-net in particle size estimation for 30 images (rock particle size distribution) was compared with the results of sieve analysis, automatic and manual modes of Split-Desktop. The results for four images are shown in **Figure 14**.

Also, a quantitative evaluation for 30 test images was carried out, using Root Mean Square Error (RMSE) (**Equation 5**). For this purpose, F_{30} and F_{80} were considered. The results achieved are shown in **Table 6**.

$$\text{RMSE} = \sqrt{\frac{\sum_{1}^{N}(X_i - Y_i)^2}{N}} \qquad (5)$$

Where:

X_i – The real (sieve size) cumulative percentage passing (F_{30} or F_{80}),

Y_i – The predicted cumulative percentage passing (F_{30} or F_{80}), using U-net or Split-Desktop,

N – The number of samples (test images).

Based on the size distribution analysis and the RMSE of F_{30} and F_{80} obtained for 30 images ((F_{30}: 0.36, 1.20), (F_{80}: 0.31, 1.24)) (see **Table 6**), the proposed algorithm based on modified U-net gives closer results to the sieve size compared to manual and automatic Split-Desktop. The existing errors most probably are related to the volume estimation based on 2D analysis, overlapping, and recognizing the floor as a particle in small sizes.

4. Discussion and Conclusions

In this research, an approach based on convolutional neural network (U-net was used and then modified) was used for rock particles edge detection and determination of fragment size distribution, using the measurement of Ferret diameter. 150 lab and field images were used for network training and 30 lab and field test images were used for network validation. The results for 30 test images were compared with the manually edge detected and the results obtained by the Split-Desktop automatic edge detection software on the same images. Based on the obtained results, there is a very good visual matching between the results achieved through the defined networks and the laboratory and field images. Also, F1-score was used to quantify the process of validation. The results show a better matching between the manually edge detected images and the outputs of networks for both laboratory and field datasets compared to the results of Split-Desktop automatic edge detection.

Also, by using RMSE, the performance of the proposed approach for fragments size distribution for laboratory images was evaluated. The obtained results showed that the RMSE for F_{30} and F_{80} are less than the RMSE for Split-Desktop manually edge detected software ((F_{30}: 0.36, 1.20), (F_{80}: 0.31, 1.24)), which once again show the better performance of the new approach over Split-Desktop software. In addition to these, it is possible to analyse a large number of images in a short time without disturbing mining operation. These advantages make this approach an efficient tool to evaluate the fragmentation caused by blasting in mines.

5. References

Abdel-Hamid, O., Deng, L. and Yu, D. (2013): Exploring convolutional neural network structures and optimization techniques for speech recognition. Interspeech, 2013, 1173-5. Available at: https://doi.org/10.21437/interspeech.2013-744.

Al-Thyabat, S., Miles, N.J. and Koh, T.S. (2007): Estimation of the size distribution of particles moving on a conveyor belt. Minerals Engineering, 20, 1, 72-83. Available at: https://doi.org/10.1016/j.mineng.2006.05.011.

Bai, F., Fan, M., Yang, H., and Dong, L. (2021): Image segmentation method for coal particle size distribution analysis. Particuology, 56, 163–170. Available at: https://doi.org/10.1016/J.PARTIC.2020.10.002

Bamford, T., Esmaeili, K. and Schoellig, A.P. (2021): A deep learning approach for rock fragmentation analysis. International Journal of Rock Mechanics and Mining Sciences, 145, 104839. Available at: https://doi.org/10.1016/j.ijrmms.2021.104839.

Bhattacharya, J. and Chandrakar, C. (1999): Comparison of three edge detection methods for image analysis of fragmented sandstones and bricks. Fragblast, 3, 3, 251-265. Available at: https://doi.org/10.1080/13855149909408049.

Bull, G., Gao, J. and Antolovich, M. (2015): Rock fragment boundary detection using compressed random features. Computer Vision, Imaging and Computer Graphics-Theory and Applications: International Joint Conference, VISIGRAPP 2014, Lisbon, Portugal, January 5-8, 2014, Revised Selected Papers 9., 273-286. Available at: https://doi.org/10.1007/978-3-319-25117-2_17.

Csurka, G., Larlus, D. and Perronnin, F. (2013): What is a good evaluation measure for semantic segmentation?. BMVC ,27, 2013, 10-5244. Available at: https://doi.org/10.5244/C.27.32.

Faramarzi, F., Mansouri, H. and Ebrahimi Farsangi, M.A. (2013): A rock engineering systems based model to predict rock fragmentation by blasting. International Journal of Rock Mechanics and Mining Sciences, 60, 82–94. Available at: https://doi.org/10.1016/J.IJRMMS.2012.12.045.

Farmer, I.W., Kemeny, J.M. and Mcdoniel, C. (1991): Analysis of rock fragmentation in bench blasting using digital image processing. 7th ISRM Congress. Available at: https://doi.org/10.1016/0148-9062(93)92003-9.

Francoeur, P. G., Masuda, T., Sunseri, J., Jia, A., Iovanisci, R. B., Snyder, I., and Koes, D. R. (2020): Three-dimensional convolutional neural networks and a crossdocked data set for structure-based drug design. Journal of Chemical Information and Modeling, 60, 9, 4200-4215. Available at: https://doi.org/10.1021/acs.jcim.0c00411.

Gallagher, E. (1976): Optoelectronic coarse particle size analysers for industrial measurement and control. Doctoral dissertation, University of Queensland.

Girdner, K. K., Kemeny, J. M., Srikant, A., and McGill, R. (1996): The split system for analyzing the size distribution of fragmented rock. Measurement of Blast Fragmentation, 101–108. Available at: https://doi.org/10.1201/9780203747919-16.

Gore, S., Mohan, A., Joshi, P., Bhosale, P., George, A., and Jagtap, J. (2022): Multiregional Segmentation of High-Grade Glioma Using Modified Deep UNET Model with Edge-Detected Multimodal MRI Images. in Lecture Notes in Networks and Systems, 631-641. Available at: https://doi.org/10.1007/978-981-16-4284-5_56.

Gu, J., Wang, Z., Kuen, J., Ma, L., Shahroudy, A., Shuai, B., Liu, T., Wang, X., Wang, G., Cai, J., and Chen, T. (2018): Recent advances in convolutional neural networks. Pattern Recognition, 77, 354-377. Available at: https://doi.org/10.1016/j.patcog.2017.10.013.

Guo, Y., Liu, Y., Oerlemans, A., Lao, S., Wu, S., and Lew, M. S. (2016): Deep learning for visual understanding: A review. Neurocomputing, 187, 27-48. Available at: https://doi.org/10.1016/j.neucom.2015.09.116.

Hamzeloo, E., Massinaei, M. and Mehrshad, N. (2014): Estimation of particle size distribution on an industrial conveyor belt using image analysis and neural networks. Powder Technology, 261, 185-190. Available at: https://doi.org/10.1016/j.powtec.2014.04.038.

Han, J.H. and Song, J.J. (2014): Statistical estimation of blast fragmentation by applying stereophotogrammetry to block piles. International Journal of Rock Mechanics and Mining Sciences, 68, 150-158. Available at: https://doi.org/10.1016/j.ijrmms.2014.02.010.

Han, J.H. and Song, J.J. (2016): Block delineation algorithm for rock fragmentation analysis. International Journal of Rock Mechanics and Mining Sciences, 82, 48-60. Available at: https://doi.org/10.1016/j.ijrmms.2015.12.005.

He, K., Zhang, X., Ren, S., and Sun, J. (2016): Deep residual learning for image recognition. Proceedings of the IEEE Computer Society Conference on Computer Vision and Pattern Recognition, 770-778. Available at: https://doi.org/10.1109/CVPR.2016.90.

Hudaverdi, T., Kuzu, C. and Fisne, A. (2012): Investigation of the blast fragmentation using the mean fragment size and fragmentation index. International Journal of Rock Mechanics and Mining Sciences, 56, 136-145. Available at: https://doi.org/10.1016/j.ijrmms.2012.07.028.

Jang, H., Kitahara, I., Kawamura, Y., Endo, Y., Topal, E., Degawa, R., and Mazara, S. (2020): Development of 3D rock fragmentation measurement system using photogrammetry. International Journal of Mining, Reclamation and Environment, 34, 4, 294-305. Available at: https://doi.org/10.1080/17480930.2019.1585597.

Karimpouli, S. and Tahmasebi, P. (2019): Segmentation of digital rock images using deep convolutional autoencoder networks', Computers and Geosciences. 126, 142-150. Available at: https://doi.org/10.1016/j.cageo.2019.02.003.

Kattenborn, T., Leitloff, J., Schiefer, F., and Hinz, S. (2021): Review on Convolutional Neural Networks (CNN) in vegetation remote sensing. ISPRS Journal of Photogrammetry and Remote Sensing, 173, 24-49. Available at: https://doi.org/10.1016/j.isprsjprs.2020.12.010.

Kemeny, J.M. (1994): Practical technique for determining the size distribution of blasted benches, waste dumps and heap leach sites. Mining Engineering, 46, 11, 1281-1284. Available at: https://doi.org/10.1016/0148-9062(95)97076-u.

Ko, Y.D. and Shang, H. (2011): A neural network-based soft sensor for particle size distribution using image analysis. Powder Technology, 212, 2, 359-366. Available at: https://doi.org/10.1016/j.powtec.2011.06.013.

Li, H., Asbjörnsson, G. and Lindqvist, M. (2021): Image process of rock size distribution using dexined-based neural network. Minerals, 11, 7, 736. Available at: https://doi.org/10.3390/min11070736.

Li, M., Wang, X., Yao, H., Saxén, H., and Yu, Y. (2022): Analysis of Particle Size Distribution of Coke on Blast Furnace Belt Using Object Detection. Processes, 10, 10, 1902. Available at: https://doi.org/10.3390/pr10101902.

Li, P., Li, J. and Wang, G. (2019): Application of Convolutional Neural Network in Natural Language Processing. 2018 15th International Computer Conference on Wavelet Active Media Technology and Information Processing, ICCWAMTIP 2018, 120-122. Available at: https://doi.org/10.1109/ICCWAMTIP.2018.8632576.

Li, Q., Cai, W., Wang, X., Zhou, Y., Feng, D. D., and Chen, M. (2014): Medical image classification with convolutional

neural network. 2014 13th International Conference on Control Automation Robotics and Vision, ICARCV, 844-848. Available at: https://doi.org/10.1109/ICARCV.2014.7064414.

Lin, C.L., Yen, Y.K. and Miller, J.D. (1993): Evaluation of a PC image-based on-line coarse particle size analyzer. Proceedings of Emerging Computer Techniques for the Mineral Industry Symposium, AIME/SME, 201-210. Available at: https://collections.lib.utah.edu/details?id=704069 (Accessed: 26 November 2023).

Lin, M., Chen, Q. and Yan, S. (2013): Network In Network. arXiv preprint arXiv:1312.4400. Available at: https://doi.org/10.48550/arXiv.1312.4400

Luo, H., Xiong, C., Fang, W., Love, P. E. D., Zhang, B., and Ouyang, X. (2018): Convolutional neural networks: Computer vision-based workforce activity assessment in construction. Automation in Construction, 94, 282-289. Available at: https://doi.org/10.1016/j.autcon.2018.06.007.

Luo, Z., Zhang, Y., Zhou, L., Zhang, B., Luo, J., and Wu, H. (2019): Micro-Vessel Image Segmentation Based on the AD-UNet Model. IEEE Access, 7, 143402–143411. Available at: https://doi.org/10.1109/ACCESS.2019.2945556.

Maerz, N., Franklin, J. and Coursen, D. (1987): Fragmentation Measurement for Experimental Blasting in Virginia. Proceedings of the 3rd Mini-Symposium on Explosives and Blasting Research (1987, Miami, FL), 56-70. Available at: https://scholarsmine.mst.edu/geosci_geo_peteng_facwork/1248.

Maerz, N.H., Palangio, T.C. and Franklin, J.A. (1996): WipFrag image based granulometry system. Measurement of Blast Fragmentation, 91–99. Available at: https://doi.org/10.1201/9780203747919-15.

Meng, F., Lu, Z., Wang, M., Li, H., Jiang, W., and Liu, Q. (2015): Encoding source language with convolutional neural network for machine translation. arXiv preprint arXiv:1503.01838. Available at: https://doi.org/10.3115/v1/p15-1003.

Mousavi, S. M., Zhu, W., Sheng, Y., and Beroza, G. C. (2019): CRED: A Deep Residual Network of Convolutional and Recurrent Units for Earthquake Signal Detection. Scientific Reports, 9, 1, 10267. Available at: https://doi.org/10.1038/s41598-019-45748-1.

Nyberg, L., Carlsson, O. and Schmidtbauer, B. (1983): Estimation of the size distribution of fragmented rock in ore mining through automatic image processing. International Measurement Conference: 24/05/1982-28/05/1982, 293-302.

Obara, B., Kozusnikova, A. and Scucka, J. (2011): Automatic identification of microcracks observed on microscopic images of coarse-grained sandstone. International Journal of Rock Mechanics and Mining Sciences, 48, 4, 681-686. Available at: https://doi.org/10.1016/j.ijrmms.2011.01.005.

Otsu, N. (1979): A threshold selection method from gray-level histograms. IEEE transactions on systems, man, and cybernetics, 9, 1, 62-66. Available at: https://cw.fel.cvut.cz/b201/_media/courses/a6m33bio/otsu.pdf.

Petersen, K., Nielsen, M., Diao, P., Karssemeijer, N., and Lillholm, M. (2014): Breast tissue segmentation and mammographic risk scoring using deep learning. Breast Imaging: 12th International Workshop, IWDM 2014, Gifu City, Japan, June 29 July 2, 2014. Proceedings 12, 88-94. Available at: https://doi.org/10.1007/978-3-319-07887-8_13.

Rahmani, H., Scanlan, C., Nadeem, U., Bennamoun, M., and Bowles, R. (2019): Automated segmentation of gravel particles from depth images of gravel-soil mixtures. Computers and Geosciences, 128, 1-10. Available at: https://doi.org/10.1016/j.cageo.2019.03.005.

Romanuke, V. V. (2019): An infinitely scalable dataset of single-polygon grayscale images as a fast test platform for semantic image segmentation. KPI Science News. Available at: https://doi.org/10.20535/kpi-sn.2019.1.157259.

Ronneberger, O., Fischer, P. and Brox, T. (2015): U-net: Convolutional networks for biomedical image segmentation. Medical Image Computing and Computer-Assisted Intervention--MICCAI 2015: 18th International Conference, Munich, Germany, October 5-9, 2015, Proceedings, Part III 18, 234-241. Available at: https://doi.org/10.1007/978-3-319-24574-4_28.

Roy, P.P. (2005): Rock blasting: effects and operations. CRC Press.

Sanchidrián, J. A., Ouchterlony, F., Moser, P., Segarra, P., and López, L. M. (2012): Performance of some distributions to describe rock fragmentation data. International Journal of Rock Mechanics and Mining Sciences, 53, 18-31. Available at: https://doi.org/10.1016/j.ijrmms.2012.04.001.

Sereshki, F., Hoseini, S.M. and Ataei, M. (2016): Blast fragmentation analysis using image processing. International Journal of Mining and Geo-Engineering (IJMG), 50, 2, 211-218. Available at: https://doi.org/10.22059/IJMGE.2016.59831.

Shamsolmoali, P., Zareapoor, M., Wang, R., Zhou, H., and Yang, J. (2019): A Novel Deep Structure U-Net for Sea-Land Segmentation in Remote Sensing Images. IEEE Journal of Selected Topics in Applied Earth Observations and Remote Sensing, 12,9, 3219-3232. Available at: https://doi.org/10.1109/JSTARS.2019.2925841.

Siddiqui, F., Shah, S. and Behan, M. (2009): Measurement of Size Distribution of Blasted Rock Using Digital Image Processing. Engineering Sciences, 20, 2. Available at: https://doi.org/10.4197/eng.20-2.4.

Sivagami, S., Chitra, P., Kailash, G. S. R., and Muralidharan, S. R. (2020): UNet Architecture Based Dental Panoramic Image Segmentation. 2020 International Conference on Wireless Communications, Signal Processing and Networking (WiSPNET), 187-191. Available at: https://doi.org/10.1109/WiSPNET48689.2020.9198370.

Sudhakar, J., Adhikari, G.R. and Gupta, R.N. (2006): Comparison of fragmentation measurements by photographic and image analysis techniques. Rock Mechanics and Rock Engineering, 39, 2, 159-168. Available at: https://doi.org/10.1007/s00603-005-0044-9.

Targ, S., Almeida, D. and Enlitic, K.L. (2016): Resnet in Resnet: Generalizing Residual Architectures. arXiv preprint arXiv:1603.08029. Available at: https://doi.org/10.48550/arXiv.1603.08029.

Thurley, M.J. (2011): Automated online measurement of limestone particle size distributions using 3D range data. Journal of Process Control, 21, 2, 254-262. Available at: https://doi.org/10.1016/j.jprocont.2010.11.011.

Thurley, M.J. and Andersson, T. (2008): An industrial 3D vision system for size measurement of iron ore green pellets using morphological image segmentation. Minerals engineering, 21,5, 405-415. Available at: https://doi.org/10.1016/j.mineng.2007.10.020.

Wang, W. (2008): Rock Particle Image Segmentation and Systems. Pattern Recognition Techniques, Technology and Applications, 197-226. Available at: https://doi.org/10.5772/6242.

Wang, W.X. (1998): Binary image segmentation of aggregates based on polygonal approximation and classification of concavities. Pattern Recognition, 31, 10, 1503-1524. Available at: https://doi.org/10.1016/S0031-3203(97)00145-3.

Wang, W.X. and Bergholm, F. (2005): Online particle size estimation on one-pass edge detection and particle shape. International Conference on Machine Learning and Cybernetics (ICMLC), 9, 5318-5323. Available at: https://doi.org/10.1109/icmlc.2005.1527883.

Weimer, D., Scholz-Reiter, B. and Shpitalni, M. (2016): Design of deep convolutional neural network architectures for automated feature extraction in industrial inspection. CIRP Annals - Manufacturing Technology, 65, 1, 417-420. Available at: https://doi.org/10.1016/j.cirp.2016.04.072.

Wu, X. and Kemeny, J.M. (1992): A segmentation method for multi-connected particle delineation. Proceedings of IEEE Workshop on Applications of Computer Vision, 240-241. Available at: https://doi.org/10.1109/ACV.1992.240305.

Xie, C., Nguyen, H., Bui, X. N., Choi, Y., Zhou, J., and Nguyen-Trang, T. (2021): Predicting rock size distribution in mine blasting using various novel soft computing models based on meta-heuristics and machine learning algorithms. Geoscience Frontiers, 12, 3, 101108. Available at: https://doi.org/10.1016/j.gsf.2020.11.005.

Yaghoobi, H., Mansouri, H., Ebrahimi Farsangi, M. A., and Nezamabadi-Pour, H. (2019): Determining the fragmented rock size distribution using textural feature extraction of images. Powder Technology, 342, 630-641. Available at: https://doi.org/10.1016/j.powtec.2018.10.006.

Yang, X., Ren, T. and Tan, L. (2020): Size distribution measurement of coal fragments using digital imaging processing. Measurement, 160, 107867. Available at: https://doi.org/10.1016/j.measurement.2020.107867.

Yang, Z., He, B., Liu, Y., Wang, D., and Zhu, G. (2021): Classification of rock fragments produced by tunnel boring machine using convolutional neural networks. Automation in Construction, 125, 103612. Available at: https://doi.org/10.1016/j.autcon.2021.103612.

Yen, Y.K., Lin, C.L. and Miller, J.D. (1998): Particle overlap and segregation problems in on-line coarse particle size measurement. Powder Technology, 98, 1, 1–12. Available at: https://doi.org/10.1016/S0032-5910(97)03405-0.

Zeng, H., Edwards, M. D., Liu, G., and Gifford, D. K. (2016): Convolutional neural network architectures for predicting DNA-protein binding. Bioinformatics, 32, 12, i121-i127. Available at: https://doi.org/10.1093/bioinformatics/btw255.

Zhang, Z., Yang, J., Ding, L., and Zhao, Y. (2012): Estimation of coal particle size distribution by image segmentation. International Journal of Mining Science and Technology, 22, 5, 739-744. Available at: https://doi.org/10.1016/j.ijmst.2012.08.026.

SAŽETAK

Određivanje raspodjele veličine stijenskih fragmenata pomoću konvolucijske neuronske mreže

Brzo i relativno točno određivanje raspodjele veličine fragmenata usitnjenoga materijala još je uvijek izazov u rudarstvu, a postojeće metode za mjerenja raspodjele nisu učinkovite. U ovome istraživanju prikazan je novi algoritam za određivanje veličine fragmenata uslijed miniranja koji se koristi tehnikom obrade slike. U novopredloženome pristupu ocrtavanje usitnjenih stijenskih fragmenata provedeno je korištenjem konvolucijske neuronske mreže. Dvije mreže načinjene su i trenirane pomoću 150 laboratorijskih i 150 terenskih slika. Također, primijenjeno je 30 laboratorijskih i 30 terenskih slika kako bi se provela validacija vizualnim putem i F1-mjerom (engl. *F1-Score*). Na istim slikama dvije laboratorijske i terenske mreže imale su F1-mjeru od 0,98 i 0,99 nasuprot 0,74 i 0,85 za dobivene rezultate pomoću automatskoga otkrivanja rubova programom Split-Desktop. Također, za određivanje raspodjele veličine fragmenata pomoću mreže na bazi laboratorijskih podataka srednja kvadratna pogreška (RMSE) za F_{30} i F_{80} iznosila je 0,31 i 0,36 odnosno 1,20 i 1,24 kod automatskoga otkrivanja rubova softverom Split-Desktop na istim slikama. To upućuje na bolja svojstva predloženoga pristupa za otkrivanje rubova stijene i raspodjelu veličine fragmenata u odnosu na automatsko otkrivanje rubova programom Split-Desktop.

Ključne riječi:
obrada slike, otkrivanje rubova stijenskih fragmenata, određivanje raspodjele veličine fragmenata, strojno učenje, konvolucijske neuronske mreže

Author's contribution

Mohamad Ali Ebrahimi Farsangi (Associate Professor of Mining Engineering, Department of Mining Engineering, Shahid Bahonar University of Kerman, Iran) and **Hamid Mansouri** (Associate Professor of Mining Engineering, Department of Mining Engineering, Shahid Bahonar University of Kerman, Iran) along with **Esmat Rashedi** (Associate Professor of Communication Engineering, Department of Electrical and Computer Engineering, Graduate University of Advanced Technology, Kerman, Iran) supervised the research work. **Elmira Sharifi**, a PhD candidate, carried out the data collection and modelling.